HOKKAIDO UNIVERSITY

Title	Excitonic properties in ZnSe/ZnSxSe1-x strained-layer superlattices by one- and two-photon spectroscopy
Author(s)	Tommasi, R.; Lepore, M.; Netti, M. C.; Catalano, I. M.; Suemune, I.
Citation	PHYSICAL REVIEW B, 49(20), 14367-14371 https://doi.org/10.1103/PhysRevB.49.14367
Issue Date	1994-05
Doc URL	http://hdl.handle.net/2115/5887
Rights	Copyright © 1994 American Physical Society
Type	article
File Information	PRB-49-20.pdf

Instructions for use

Excitonic properties in ZnSe/ZnS$_x$Se$_{1-x}$ strained-layer superlattices by one- and two-photon spectroscopy

R. Tommasi,* M. Lepore, M. C. Netti, and I. M. Catalano

*Dipartimento di Fisica – Gruppo Nationale di Elettronica Quautistica e Plasmi, Università di Bari,
via Orabona 4, I-70126 Bari, Italy*

I. Suemune

Research Institute for Electronics Science, Hokkaido University, Sapporo, Japan

Excitonic properties of ZnSe/ZnS$_{0.18}$Se$_{0.82}$ strained-layer superlattices have been investigated by means of one- and two-photon absorption spectroscopy. Heavy- and light-hole excitons associated with $n = 1,2$ subbands have been observed and experimental evidence of $2s$ states in these systems has been obtained. Experimental exciton transition energies have been found to be in good agreement with theoretical predictions considering strain and confinement effects. The different selection rules governing linear and nonlinear absorption processes have been verified and some violations of them have been observed. Furthermore, exciton binding energy has been measured and compared with the result of a recent theoretical model.

Recently the physics of wide-band-gap ZnSe-based semiconductor heterostructures has been the object of both theoretical[1] and experimental investigations.[2] This growing interest has been due to many technological applications that have been devised for these compounds and to the excitonic properties that are expected to play a dominant role. In particular, ZnSe/ZnS$_x$Se$_{1-x}$ strained-layer superlattices (SLS's) have shown to be good candidates for designing efficient blue-light-emitting diodes and blue-injection lasers.[3] In fact, it is well known that in ZnSe compounds the exciton binding energy (E_b) is larger than in III-V compounds ($E_b \simeq 20$ meV for ZnSe bulk and $E_b \simeq 4$ meV in GaAs bulk). In order to investigate some ZnSe/ZnS$_x$Se$_{1-x}$ SLS fundamental properties we have performed one- and two-photon spectroscopic measurements. More precisely, the aims of the present work have been as follows: (i) to study the excitonic transitions in some ZnSe/ZnS$_x$Se$_{1-x}$ SLS samples; (ii) to verify the different parity selection rules that are involved in one- and two-photon absorption (OPA, TPA) processes in these compounds; (iii) to evaluate the excitonic binding energy by measuring the difference in energy between the $1s$ and $2p$ excitonic states and compare it with the results of a recent theoretical model.[4]

In order to fulfill the above-mentioned aims two different samples of ZnSe/ZnS$_{0.18}$Se$_{0.82}$ SLS's have been investigated. The SLS's concerned were grown by atmospheric-pressure metalorganic chemical vapor deposition on (100) GaAs substrates using diethylzinc, diethylselenide, and diethylsulfide at the growth temperature of 515 °C. Samples had equal well and barrier thickness (100 Å for the S100 sample and 37 Å for the S37 one). The sulfur composition of 18% was chosen in order to minimize misfit dislocations. The strain was determined to be $\tau = 24\%$ for S100 and $\tau = 0.08\%$ for S37 by independent Raman measurements.

The linear and nonlinear absorptions were studied by measuring the one- and two-photon absorption-induced photoluminescence excitation spectra (OPA-PLE and TPA-PLE) in the energy range $2.817 \leq \hbar\omega_1(\hbar\omega_2) \leq 2.883$ eV for S100 and $2.837 \leq \hbar\omega_1(2\hbar\omega_2) \leq 2.917$ eV for S37. The detection energy was set at the fundamental exciton energy (E_{11h}^{1s}), which was independently determined by photoluminescence (PL) measurements. (We shall use the notation $E_{ijh(l)}^q$ where i is the electron subband, j the hole subband, h and l stand for heavy and light hole, respectively, and q indicates the state of the exciton $1s$, $2s$, $2p$, etc.)

All the spectra were obtained at $T = 10$ K. The excitation source of the PL, OPA-PLE, and TPA-PLE spectra was a 10-Hz Quantel Datachrome dye laser (pulse duration of 9 nsec, tuning accuracy 2 Å, maximum peak power of about 20 MW/cm^2 after focusing) pumped by the second harmonic of a Nd:YAG laser (where YAG is yttrium aluminum garnet), and equipped with a low-pressure H$_2$ Raman shifter to give the near-infrared radiation employed for TPA measurements. In particular for PL and PLE measurements Stilbene dye was used, while DCM dye was employed for TPA measurements. The emitted radiation was detected perpendicularly to the excitation radiation by an S-20 extended-response photomultiplier tube, while the incident beam was monitored by a fast-response photodiode. Both signals were stored and processed by a computer data-acquisition system. The signal-to-noise ratio was better than 200:1 for each run. In the TPA measurements to reduce the effects of fluctuations in the input beam intensity, a ratio of the photomultiplier signal to the second power of the monitor signal was used. Moreover, the quadratic behavior of the detected luminescence signal versus the excitation intensity was checked at each experimental point and, for each of them, different measurement runs were carried

out and quadratic regression analysis was performed. Slope 2 fits the experimental points within 3% at all wavelengths. The OPA-PLE and TPA-PLE spectra were obtained by measuring the luminescence signal every 2 meV on average.

In Fig. 1(a), the PL and OPA-PLE spectra for the S100 sample are reported. The PL (excited at $\hbar\omega = 2.92$ eV) shows a strong peak at 2.814 eV with a full width at half maximum (FWHM) of 10 meV that has been attributed
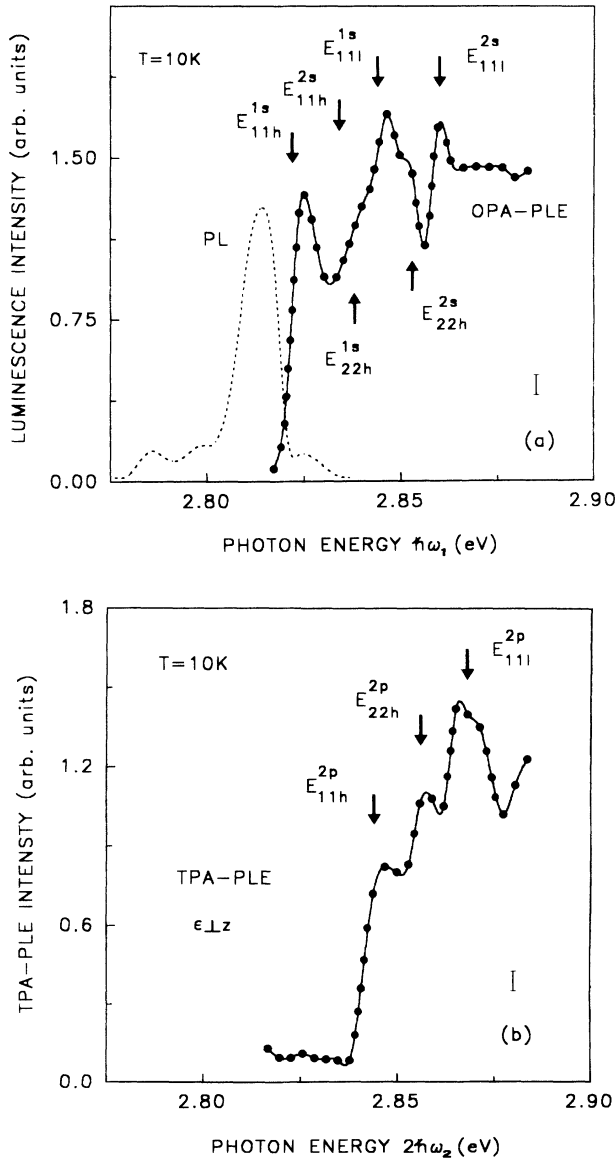

FIG. 1. (a) Photoluminescence (PL) and one-photon absorption-induced photoluminescence excitation (OPA-PLE) spectra of the S100 sample at $T = 10$ K. The arrows indicate the theoretical excitonic transition energies reported in Table I calculated taking into account strain and confinement effects. (b) Two-photon absorption photoluminescence excitation (TPA-PLE) spectrum of the same sample at $T = 10$ K obtained in the $\epsilon \perp z$ electric-field polarization. The arrows indicate the TPA-allowed transitions. The vertical error bars deriving from the signal-to-noise ratio and the regression analysis of the experimental points are indicated.

to the fundamental excitonic state E_{11h}^{1s}. The OPA-PLE spectrum was obtained by monitoring this photoluminescence intensity peak. It shows strong excitonic structures superimposed on the typical superlattice absorption continuum, in agreement with theoretical predictions of Ref. 5 in which the variational method in the effective-mass approximation has been employed to calculate the two-photon transition rate of discrete excitonic states. The two main peaks at 2.825 and 2.846 eV have been ascribed to the E_{11h}^{1s} and E_{11l}^{1s} exciton transitions, respectively. (It may be noted that the Stokes shift between the E_{11h}^{1s} peak in PL and PLE spectra may reflect inhomogeneities in layer thicknesses.) These attributions have been done in agreement with the selection rules governing OPA processes and the theoretical predictions obtained by using the model of Ref. 6. This evaluation considers the strain and confinement effects by assuming a valence-to-conduction band offset ratio equal to 95:5. The results are reported in Table I. The faint shoulder observed at 2.838 eV can be ascribed to the E_{22h}^{1s} transition. In addition this structure can also be due to the E_{11h}^{2s} transition in agreement with the results of a recent model,[4] based on a heuristic approach. The main aim of this simple method, which is developed in the framework of the fractional space, is to obtain, with good accuracy, the exciton binding energy with an analytical expression, free of any adjustable parameters. The evaluation of $E_{11h}^{2s} - E_{11h}^{1s}$ has been done as a function of the spatial dimension parameter α, which defines the fractional dimension and describes the degree of anisotropy of the electron-hole interaction, by using the following relation:[4]

$$\frac{E^{2s} - E^{1s}}{E_0^*} = \frac{16\alpha}{(\alpha^2 - 1)^2} , \qquad (1)$$

where E_0^* is the mean value of the effective Rydberg constant and

$$\alpha = 3 - \exp(L_w^* / 2a_0^*) , \qquad (2)$$

with L_w^* representing the spatial extension of the particle motion in the growth direction of the SLS and a_0^* the mean value of the Bohr radius.[4] In the present case α is equal to 2.951 for C1-HH1, 2.958 for C1-LH1, and 2.952 for C2-HH2, respectively, due to the vanishing discontinuity in the conduction band (where $\alpha = 3$ or 2 for the three-dimensional and bidimensional case, respectively).

TABLE I. Theoretical and experimental energy positions of OPA-PLE exciton transitions for the S100 sample. For the physical parameter values employed in the calculations see Ref. 16.

Transition	Theor. (eV)	Expt. (eV)
E_{11h}^{1s}	2.824	2.825
E_{11h}^{2s}	2.838	2.838
E_{11l}^{1s}	2.843	2.846
E_{11l}^{2s}	2.857	2.862
E_{22h}^{1s}	2.840	2.838
E_{22h}^{2s}	2.854	2.853

The shoulder at 2.853 eV and the better-defined structure at 2.862 eV have been ascribed to the E^{2s}_{22h} and the E^{2s}_{11l} transition, respectively. These are the first experimental observations of these states in II-VI SLS's to our knowledge and the presence of peaks for the $2s$ states of C1-HH1 and C1-LH1 excitons is in agreement with the theoretical results of Ref. 7, in which the Coulomb coupling between excitons belonging to different subbands, and in particular the Coulomb coupling with the exciton continuum, has been shown to be very important in determining the exciton properties. In fact, the exciton Coulomb interaction with the continuum of other excitonic series increases the binding energy and the oscillator strength of C1-HH1 and C1-LH1 excitons. This increase is greater for light-hole excitons and it occurs for $1s$ and $2s$ excitons. The exchange in the energy position of the E^{1s}_{11l} and E^{2s}_{11h} (as compared to the energy levels of unstrained structures) is due to the lower energy displacement caused by the strain for the HH subbands with respect to the LH one.

In Fig. 1(b) the TPA-PLE spectrum of the S100 sample has been reported. In the experimental configuration employed here, the polarization vector of the electric field (ϵ) was perpendicular to the sample growing axis (z). In this polarization configuration, the TPA processes involve final $2p$ excitonic states for the $\Delta i = 0$ transitions, while those between the $1s$ states are forbidden by the parity selection rules holding for TPA transitions. Hence, the excitonic structures in the TPA-PLE spectrum at 2.846, 2.858, and 2.867 eV have been ascribed to the E^{2p}_{11h}, E^{2p}_{22h}, and E^{2p}_{11l} transitions, respectively. Also in this case, the displacement in the energy position of the E^{2p}_{11l} and E^{2p}_{22h} (as compared to the energy levels of unstrained structures) is due to the lower energy displacement caused by the strain for the HH subbands with respect to the LH one, as for E^{1s}_{11l} and E^{2s}_{11h}. In addition, it must be pointed out that the E^{2p}_{11l} is more evident than E^{2p}_{11h} due to the continuum effect that is stronger on light-hole excitons than on heavy-hole ones, as theoretically predicted in Ref. 5. These results further confirm the experimental evidence of p excitonic states in different III-V quantum-well systems[8,9] and in a ZnSe/ZnS superlattices sample[10] in TPA experiments when the $\epsilon \perp z$ configuration is adopted.

It is important to note that by comparing the TPA-PLE and the OPA-PLE spectra it is possible to evaluate the energy difference between the $1s$ and $2p$ exciton states. In particular $\Delta(E^{2p}_{11h} - E^{1s}_{11h}) = \Delta(E^{2p}_{11l} - E^{1s}_{11l}) = 21 \pm 2$ meV. It is interesting to note that the energy separation is equal for the light- and heavy-hole $n = 1$ exciton as in the case of a GaAs-Al$_x$Ga$_{1-x}$As QW.[8] Moreover, $\Delta(E^{2p}_{22h} - E^{1s}_{22h}) = 20 \pm 2$ meV. From the measured splitting between the $1s$ and $2p$ excitons, it is possible to estimate the exciton binding energy using the three-dimensional limit for the $2p$ exciton binding energy ($\frac{1}{4}E^*_0$), as reported by Matsuura and Shinozuka,[11] since the α values previously calculated for the involved transitions are nearly equal to 3. In so doing the exciton binding energy results to be equal to 26 ± 2 meV. This value is in agreement with the theoretical results obtained using Eq. (21) of Ref. 4,

$$E_b = \frac{E^*_0}{\left[1 - \frac{1}{2}\exp\frac{(2/K_b + L^*_w)}{2a^*_0}\right]^2} , \qquad (3)$$

where K_b is the characteristic wave vector and the other symbols have the meaning previously indicated. The binding energy does not result much higher than the ZnSe bulk value, probably due to the vanishing conduction-band offset that reduces the confinement effect.

Before discussing the results of the second sample (S37), it is important to note that this one has allowed us to better resolve the different optical transitions (especially $2s$ states) thanks to its lower well thickness (37 Å). As is well known, smaller thickness increases the energy separation between quantized levels. In this case, the α value is 2.912 for C1-HH1 and 2.927 for C1-LH1 transitions.
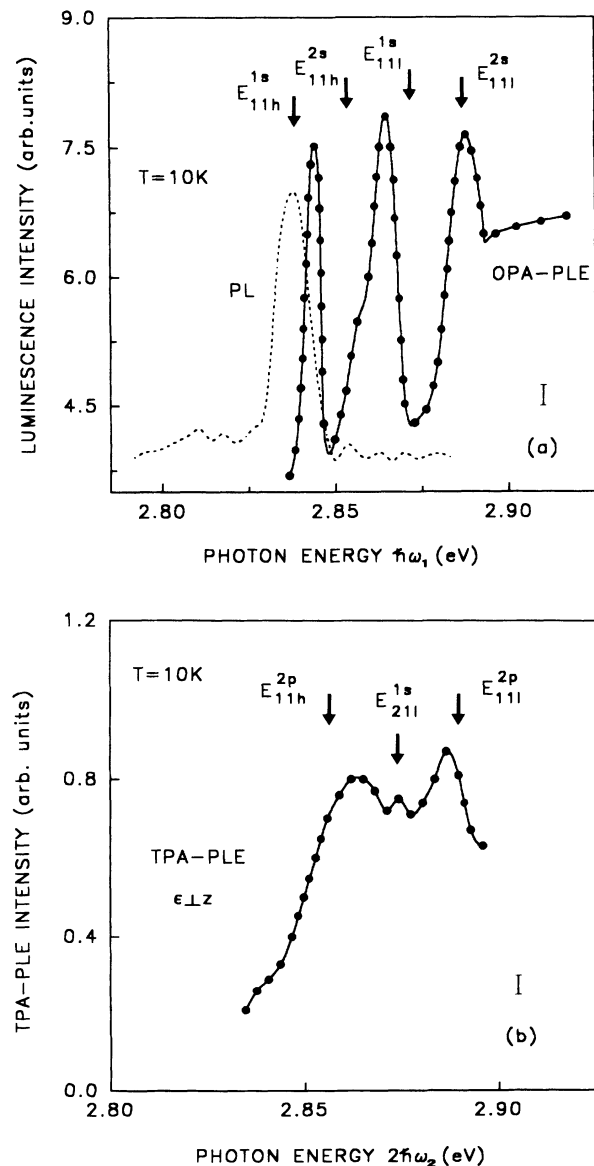

FIG. 2. As Fig. 1 for the S37 sample.

TABLE II. The same as Table I for the S37 sample.

Transition	Theor. (eV)	Expt. (eV)
E_{11h}^{1s}	2.838	2.843
E_{11h}^{2s}	2.853	2.859
E_{11l}^{1s}	2.872	2.866
E_{11l}^{2s}	2.887	2.885

In Fig. 2(a) the PL and the OPA-PLE spectra for the S37 sample are reported. The PL spectrum has been excited at the same energy as for the S100 sample and shows the fundamental excitonic peak (E_{11h}^{1s}) at 2.837 eV with FWHM of 10 meV. Analogously to the S100 sample, the OPA- and TPA-PLE have been obtained by monitoring this emission. The peaks at 2.843 and 2.866 eV have been ascribed to the E_{11h}^{1s} and E_{11l}^{1s} excitons, respectively. In this case the Stokes shift for the E_{11h}^{1s} peak is around 6 meV. The shoulder at 2.859 eV has been attributed to the E_{11h}^{2s} exciton in agreement with the theoretical results of Ref. 4. Finally, the peak at 2.885 eV is due to E_{11l}^{2s}. This attribution has been made in an analogous way by using Eq. (1) and, as expected, the excitonic structures are better defined due to the smaller well thickness. For this sample, the larger energy separation between quantized levels causes these attributions to be unambiguous because no other transition is placed in this energy range. In Table II, theoretical calculations of optical transition energies by the model of Ref. 6 are reported together with the experimental data and also for this sample a good agreement has been obtained. In Fig. 2(b) the TPA-PLE spectrum of the S37 sample is shown. The general behavior is similar to that of the S100 sample, with the optical transition energies placed at higher values with respect to the OPA-PLE spectrum. The structures at 2.865 and 2.888 eV have been ascribed to the E_{11h}^{2p} and E_{11l}^{2p} excitons. In this case, $\Delta(E_{11h}^{2p} - E_{11h}^{1s}) = \Delta(E_{11l}^{2p} - E_{11l}^{1s}) = 22 \pm 2$ meV and the exciton binding energy is equal to 27 ± 2 meV, in agreement with the theoretical results also for this sample. This confirms the validity of the approach of Ref. 6 for hetero-structures with well thickness both comparable to and greater than the exciton Bohr radius.[12] In addition, the faint structure at 2.874 eV can be attributed to E_{21l}^{1s} transitions, notwithstanding the fact that this transition should occur only in the $\epsilon \| z$ configuration. In our case, this can be due to slight deviations of experimental conditions from he $\epsilon \perp z$ configuration that induce electric-field components along the z axis different from zero. The occurrence of this component is also confirmed from the behavior of the spectrum in Fig. 2(b). This, indeed, is mixed between the slopes for $\epsilon \perp z$ and $\epsilon \| z$ configurations. In fact, the spectrum shows an increase for energies lower than the E_{11h}^{2p} transition and then becomes flat. Furthermore, some authors[13] have noted that for short-period superlattices with vanishing conduction-band offset also transitions with $\Delta i \neq 0$ are possible for $\epsilon \perp z$.

It can also be pointed out that the comparison between PL and OPA-PLE measurements has allowed us to obtain information on the structural quality of the samples. In fact, in Figs. 1(a) and 2(a) the homogeneous broadening of the PL line with respect to the OPA-PLE related peaks indicates the presence of interface defects in agreement with the experimental results of Ref. 14. In addition, it is worth noting that the present α values, nearly equal to 3, confirm the controversial character (type I or II) of these heterostructures. In fact, as reported in Ref. 15, 3 is the boundary between the α values typical of type-I ($\alpha < 3$) and type-II structures ($\alpha > 3$).

In conclusion, several excitonic transitions associated with both heavy and light holes have been observed in ZnSe/ZnS$_x$Se$_{1-x}$SLS's. Experimental evidence of excitons associated with higher-order index subbands and 2s states has been obtained. The general validity of the parity selection rules for OPA and TPA processes has been verified, with some violations of them. Moreover, the exciton binding energy has been determined in agreement with the results of a recent theoretical model.

*Present address: Laboratoire d'Optique Quantique du CNRS, Ecole Polytechnique, 91128 Palaiseau Cedex, France.

[1]C. Mailhiot and D. L. Smith, Solid State Mater. Sci. B 16, 131 (1990).

[2]A. V. Nurmikko and R. L. Gunshor, Phys. Status Solidi B 173, 291 (1992).

[3]K. Nakanishi, I. Suemune, H. Masato, Y. Kuroda, and M. Yamanishi, Appl. Phys. Lett. 59, 1401 (1991).

[4]H. Mathieu, P. Lefebvre, and P. Christol, Phys. Rev. B 46, 4092 (1992).

[5]A. Pasquarello and A. Quattropani, Superlatt. Microstruct. 9, 157 (1991).

[6]K. Shazad, D. J. Olego, C. G. Van der Walle, and D. A. Cammack, J. Lumin. 46, 109 (1990).

[7]L. C. Andreani and A. Pasquarello, Europhys. Lett. 6, 259 (1988).

[8]I. M. Catalano, A. Cingolani, M. Lepore, R. Cingolani, and K. Ploog, Phys. Rev. B 40, 1312 (1989).

[9]I. M. Catalano, A. Cingolani, M. Lepore, R. Cingolani, and K. Ploog, Solid State Commun. 71, 217 (1989); Phys. Rev. B 41, 12 397 (1990); Nuovo Cimento D 12, 217 (1990).

[10]F. Minami, K. Yoshida, J. Gregus, and K. Inoue, in Proceedings of the 2nd International Meeting on Optics of Excitons in Confined Systems, Giardini Naxos, Italy, 1991, edited by A. D'Andrea, R. Del Sole, R. Girlanda, and A. Quattropani, IOP Conf. Proc. No. 213 (Institute of Physics and the Physical Society, Bristol, England, 1992), p. 249.

[11]M. Matsuura and Y. Shinozuka, J. Phys. Soc. Jpn. 53, 3138 (1984).

[12]P. Lefebvre, P. Christol, and H. Mathieu, Phys. Rev. B 46, 13 603 (1992).

[13]L. Quiroga, F. J. Rodriguez, A. Camacho, and C. Tejedor, Phys. Rev. B 40, 11 198 (1990).

[14]L. Tapfer, W. Stolz, and K. Ploog, J. Appl. Phys. 66, 3217

(1989).

[15]P. Lefebvre, P. Christol, and H. Mathieu, in *Proceedings of the Third International Conference on Optics of Excitons in Confine Systems, Montpellier, France, 1993*, edited by G. Bastard and B. Gil (Les Editions de Physique, Les Ulis, Cedex,

France, 1993).

[16]M. Sondergeld *et al.*, in *Physics of II-VI and I-VII Compounds, Semimagnetic Semiconductors*, edited by O. Madelung, Landolt-Börnstein, New Series, Group III, Vol. 17, Pt. B (Springer-Verlag, Berlin, 1982).